

# Microstructure Analysis of Selected Platinum Alloys

doi:10.1595/147106711X554008

<http://www.platinummetalsreview.com/>

**By Paolo Battaini**

8853 SpA, Via Pitagora 11, I-20016 Pero, Milano, Italy;

*Metallographic analysis can be used to determine the microstructure of platinum alloys in order to set up working cycles and to perform failure analyses. A range of platinum alloys used in jewellery and industrial applications was studied, including several commonly used jewellery alloys. Electrochemical etching was used to prepare samples for analysis using optical metallography and additional data could be obtained by scanning electron microscopy and energy dispersive spectroscopy. The crystallisation behaviour of as-cast alloy samples and the changes in microstructure after work hardening and annealing are described for the selected alloys.*

## Introduction

Optical metallography is a widely used investigation technique in materials science. It can be used to describe the microstructure of a metal alloy both qualitatively and quantitatively. Here, the term 'microstructure' refers to the internal structure of the alloy as a result of its composing atomic elements and their three-dimensional arrangement over distances ranging from 1 micron to 1 millimetre.

Many alloy properties depend on the microstructure, including mechanical strength, hardness, corrosion resistance and mechanical workability. Metallography is therefore a fundamental tool to support research and failure analysis (1–3). This is true for all industrial fields where alloys are used. A great deal of literature is available on the typical methods used in optical metallography (4–6).

A large amount of useful information is available in the literature for precious metals in general (7–10). However, there is less information specifically focussed on platinum and its alloys.

The present work aims to give some examples of platinum alloy microstructures, both in the as-cast and work hardened and annealed conditions, and to demonstrate the usefulness of optical metallography in describing them. This paper is a revised and updated account of work that was presented at the

24th Santa Fe Symposium® on Jewelry Manufacturing Technology in 2010 (11).

### Materials and Methods

A wide variety of platinum alloys are used in jewellery (12–18) and industrial applications (10, 19–21). Different jewellery alloys are used in different markets around the world, depending on the specific country's standards for precious metal hallmarking. The alloys whose microstructures are discussed here are listed in [Table I](#). These do not represent all the alloys available on the market, but were chosen as a representative sample of the type of results that can be obtained using metallographic techniques. The related Vickers microhardness of each alloy sample, measured on the metallographic specimen with a load of 200 gf (~2 N) in most cases, is given for each microstructure.

If metallographic analysis is aimed at comparing the microstructure of different alloys in their as-cast

condition, the initial samples must have the same size and shape. Mould casting or investment casting can produce different microstructures, with different grain sizes and shapes, depending on parameters such as mould shape, size and temperature, the chemical composition of the mould, etc. Therefore, whenever possible, the specimens for the present study were prepared under conditions which were as similar as possible, including the casting process. The specimens were prepared by arc melting and pressure casting under an argon atmosphere to the shape shown in [Figure 1](#). A Yasui & Co. Platinum Investment was used, with a final flask preheating temperature of 650°C. The captions of the micrographs specify whether the original specimen is of the type described above.

The preparation of the metallographic specimens consists of the following four steps: sectioning, embedding the sample in resin, polishing the metallographic section, and sample etching for microstructure

Table I

### Selected Platinum Alloys

Composition, wt%	Melting range <sup>a</sup> , °C	Vickers microhardness <sup>b</sup> , HV <sub>200</sub>
Pt	1769	65 <sup>c</sup>
Pt-5Cu <sup>d</sup>	1725–1745	130
Pt-5Co <sup>d</sup>	1750–1765	130
Pt-5Au <sup>d</sup>	1740–1770	127
Pt-5Ir <sup>d</sup>	1780–1790	95
Pt-5Ru <sup>d</sup>	1780–1795	125
70Pt-29.8Ir <sup>e</sup>	1870–1910	330
70Pt-30Rh	1910 <sup>f</sup>	127
90Pt-10Rh	1830–1850 <sup>f</sup>	95
60Pt-25Ir-15Rh	n/a	212

<sup>a</sup>Some melting ranges are not given as they have not yet been reported

<sup>b</sup>The microhardness value refers to the microstructure of samples measured in this study and reported in the captions of the Figures

<sup>c</sup>HV<sub>100</sub>

<sup>d</sup>These alloys are among the most common for jewellery applications. Where it is not specified, it is assumed that the balance of the alloy is platinum

<sup>e</sup>This alloy composition is proprietary to 8853 SpA, Italy

<sup>f</sup>Solidus temperature

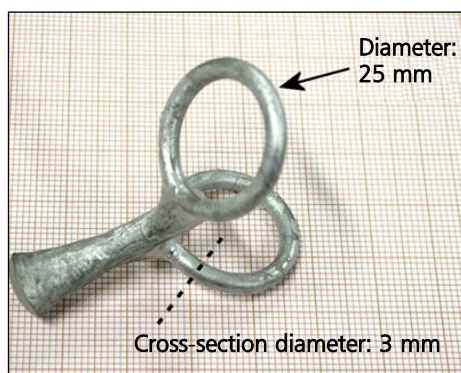


Fig. 1. General shape of specimens prepared by investment casting for this study. The microstructures of different alloys obtained by investment casting can be compared, provided that the specimens have the same size and shape. The dashed line shows the position of the metallographic sections examined in these samples

detection. The detailed description of these steps will not be given here, as they have been discussed in other works (4–10).

Further advice relevant to platinum alloys was given in the 2010 Santa Fe Symposium paper (11) and in this Journal (22). In these papers, procedures for the metallographic analysis of most platinum alloys are described. The samples for the present study were prepared by electrolytic etching in a saturated solution of sodium chloride in concentrated hydrochloric acid (37%) using an AC power supply, as described previously (22).

### Microstructures of the Platinum Alloys

In this section the microstructures of the selected platinum alloys in different metallurgical conditions are presented. As already stated, this selection is a representative sample and not a complete set of the platinum alloys which are currently on the market.

#### As-Cast Microstructures: Metallography of Crystallisation

Examination of the as-cast microstructures shows the variation in size and shape of the grains in different platinum alloys. However, a noticeable dendritic grain structure is quite common. The largest grain size was found in platinum with 5 wt% copper (Pt-5Cu) (Figure 2) and platinum with 5 wt% gold (Pt-5Au) (Figure 3), with sizes up to 1 mm and 2 mm, respectively. The Pt-5Au alloy sample also shows shrinkage porosity between the dendrites. The core of the dendritic grains showed a higher concentration of the element whose melting temperature was the highest in both cases. This behaviour, known as 'microsegregation', has been widely described (12, 23, 24). Electrolytic etching tended to preferentially dissolve the interdendritic copper- or gold-rich regions, respectively. In a platinum with 5 wt% iridium (Pt-5Ir) alloy (Figure 4), since iridium has the higher melting temperature, the dendritic crystals were enriched in iridium in the first solidification stage.

It is important to point out that the higher or lower visibility of microsegregation within the dendrites is not directly related to the chemical inhomogeneity, but to the effectiveness of the electrolytic etching in

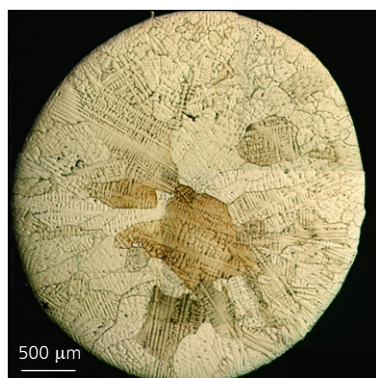


Fig. 2. As-cast Pt-5Cu alloy showing dendritic grains with copper microsegregation (sample shape as in Figure 1; flask temperature 650°C; microhardness  $130 \pm 4$  HV<sub>200</sub>)

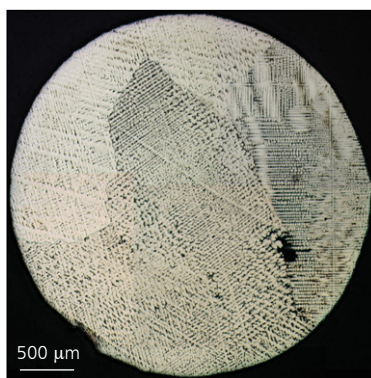


Fig. 3. As-cast Pt-5Au alloy showing shrinkage porosity between the dendrites (sample shape as in Figure 1; flask temperature 650°C; microhardness  $127 \pm 9$  HV<sub>200</sub>)

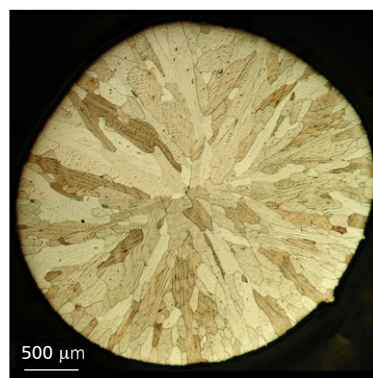


Fig. 4. As-cast Pt-5Ir alloy with columnar grains (sample shape as in Figure 1; flask temperature 650°C; microhardness  $95 \pm 2$  HV<sub>200</sub>)



revealing it. For example, the microsegregation in the platinum with 5 wt% cobalt (Pt-5Co) alloy is hardly visible in **Figure 5**, despite being easily measurable by other techniques (24).

Scanning electron microscopy (SEM) and energy dispersive spectroscopy (EDS) are very effective in showing the presence of microsegregation. **Figure 6** shows an as-cast sample of a platinum with 25 wt% iridium and 15 wt% rhodium alloy (60Pt-25Ir-15Rh). The SEM backscattered electron image is shown in **Figure 7**. The EDS maps in **Figures 8–10** give the elemental distribution on the etched surface. If the maps were obtained on the polished surface the approximate concentration of each element may be different due to the etching process and a possible preferential dissolution of different phases of the alloy.

However, because EDS is a semi-quantitative method, it can only give the general distribution of the elements on the metallographic section. It is worthwhile remembering that metallographic preparation reveals only a few microstructural features. By changing the preparation or the observation technique, some microstructural details may appear or become more clearly defined, while others remain invisible.

The melting range of the alloy and the flask pre-heating temperature affect the size and shape of grains significantly. In order to decrease the dendritic size and obtain a more homogeneous microstructure, the temperature of the material containing the solidifying alloy is lowered as much as possible. The effectiveness of such an operation is, however, limited by

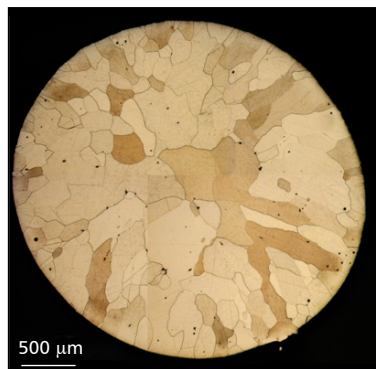


**Fig. 5.** As-cast Pt-5Co alloy with small gas porosity (sample shape as in **Figure 1**; flask temperature 650°C; microhardness  $130 \pm 6 \text{ HV}_{200}$ )

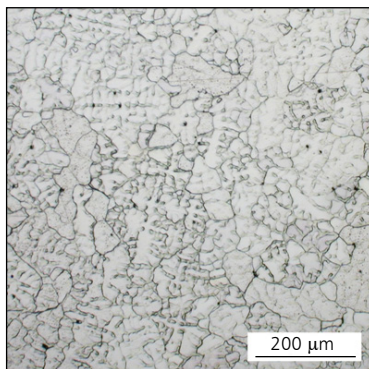


**Fig. 6.** 60Pt-25Ir-15Rh alloy cast in a copper mould. From the transverse section of an ingot (microhardness  $212 \pm 9 \text{ HV}_{200}$ )

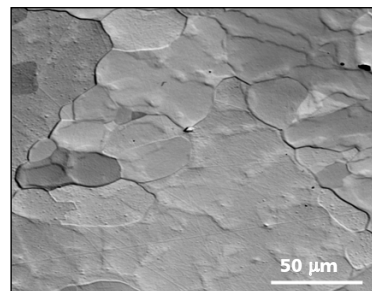


**Fig. 7.** 60Pt-25Ir-15Rh alloy: scanning electron microscopy (SEM) backscattered electron image of the etched sample. The sample is the same as that shown in **Figure 6**

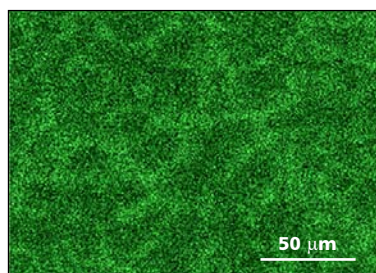


**Fig. 8.** 60Pt-25Ir-15Rh alloy: energy dispersive spectroscopy (EDS) platinum map acquired on the surface seen in **Figure 7**, showing the platinum microsegregation. The network of high platinum content shows this approximate composition (wt%): 72Pt-14Ir-14Rh

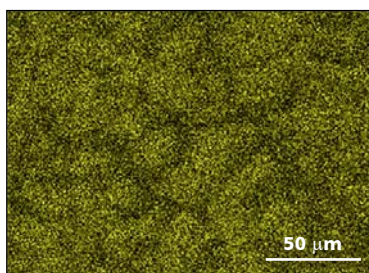


**Fig. 9.** 60Pt-25Ir-15Rh alloy: energy dispersive spectroscopy (EDS) iridium map acquired on the surface seen in **Figure 7**. The iridium concentration is lower where that of platinum is higher

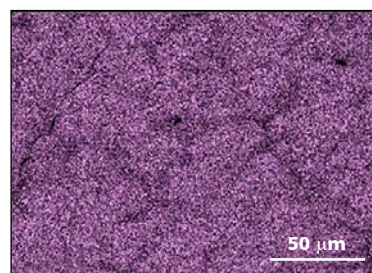


**Fig. 10.** 60Pt-25Ir-15Rh alloy: energy dispersive spectroscopy (EDS) rhodium map acquired on the surface seen in **Figure 7**. The rhodium distribution follows the behaviour of iridium. The zones of higher iridium and rhodium content show this approximate composition (wt%): 55Pt-28Ir-17Rh

the melting range and by the chemical composition of the alloy. An example of the flask temperature effect is shown in **Figure 11** for Pt-5Ir poured into a flask with a final preheating temperature of 890°C. This microstructure is to be compared with that in **Figure 4**, in which a flask preheating temperature of 650°C was used.

A smaller grain size was observed in the platinum with 5 wt% ruthenium (Pt-5Ru) alloy, which showed a more equiaxed grain (**Figure 12**) with a grain size of about 200 µm. The addition of ruthenium led to finer grains in the platinum alloy.

Pouring the alloy in a copper mould produces a smaller grain size due to the high cooling rate, as visible in **Figure 6** and **Figures 13–15**. In this case,

the high iridium and rhodium content also contributed to the lower grain size in the as-cast sample.

Homogenising thermal treatments result in a microstructural change. Comparing **Figure 16** with **Figure 17** highlights a reduction in microsegregation in Pt-5Cu as a consequence of a homogenisation treatment performed at 1000°C for 21 hours.

### Work Hardened and Annealed Microstructures: Metallography of Deformation and Recrystallisation

Optical metallography can reveal the changes in microstructure that occur after work hardening and recrystallisation thermal treatments and allows recrystallisation diagrams like the one in **Figure 18** to

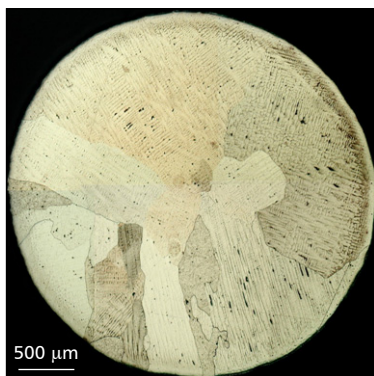


**Fig. 11.** As-cast Pt-5Ir alloy (sample shape as in **Figure 1**; flask temperature 890°C; microhardness  $105 \pm 2$  HV<sub>200</sub>)

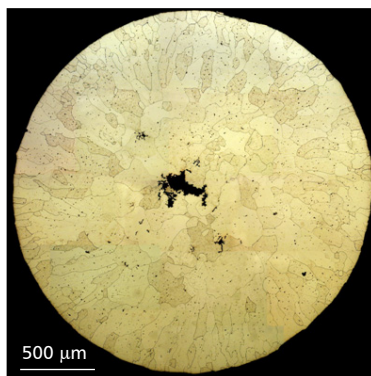


**Fig. 12.** As-cast Pt-5Ru alloy showing shrinkage porosity at the centre of the section (sample shape as in **Figure 1**; flask temperature 650°C; microhardness  $125 \pm 5$  HV<sub>200</sub>)

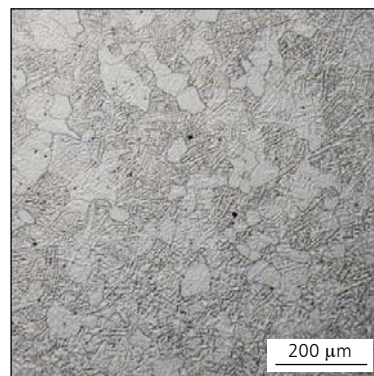


**Fig. 13.** 70Pt-29.8Ir alloy: cast in a copper mould. From an ingot transverse section. A high iridium content contributes to grain refinement (microhardness  $330 \pm 4$  HV<sub>200</sub>)

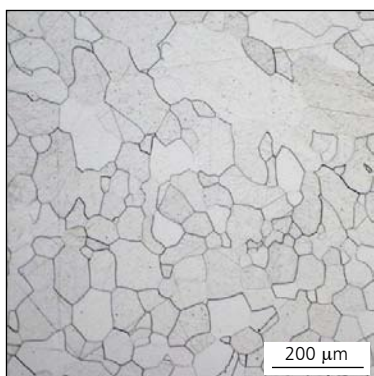


**Fig. 14.** 70Pt-30Rh alloy: cast in a copper mould. From the transverse section of an ingot. A high rhodium content enhances the grain refinement (microhardness  $127 \pm 9$  HV<sub>200</sub>)

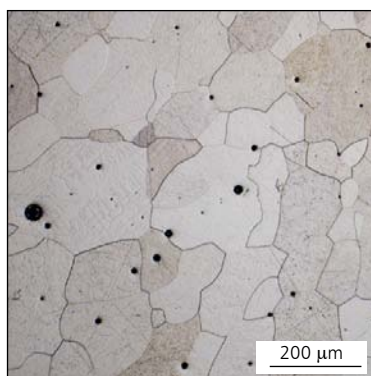


**Fig. 15.** 90Pt-10Rh alloy: cast in a copper mould. From the transverse section of an ingot. The gas porosity is visible (microhardness  $95 \pm 5$  HV<sub>200</sub>)

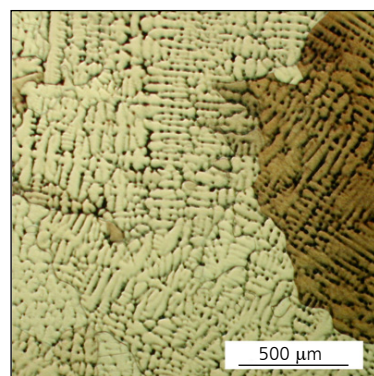


**Fig. 16.** Higher-magnification image of as-cast Pt-5Cu alloy showing dendritic grains with copper microsegregation (microhardness  $130 \pm 4$  HV<sub>200</sub>). Compare with **Figure 17**



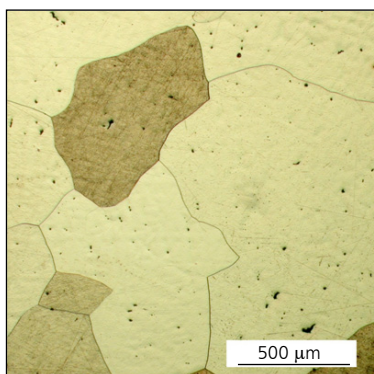


Fig. 17. Microstructure of Pt-5Cu alloy after thermal treatment at 1000°C for 21 hours. The micro-segregation of copper is reduced (micro-hardness  $120 \pm 4 \text{ HV}_{200}$ ). Compare with Figure 16

be drawn. This makes it a valuable aid in setting up working cycles. It is necessary to establish the right combination of plastic deformation and annealing treatment in order to restore the material's workability. This allows suitable final properties to be achieved.

An example of the changes in microstructure after various stages of work hardening and annealing is shown in Figure 19 for the 60Pt-25Ir-15Rh alloy. This can be compared to the as-cast structure shown in Figure 6.

Drawn wires show a very different microstructure along the drawing (longitudinal) direction in comparison to the transverse direction (Figures 20–22 for

Pt-5Au). However, after annealing, the microstructure becomes homogeneous and the fibres formed after to the drawing procedure are replaced by a recrystallised microstructure (Figures 23 and 24). Using the techniques described elsewhere (11), analyses can be performed even on very thin wires, as shown in Figure 25 for a platinum 99.99% wire of 0.35 mm diameter.

It is worth pointing out that some binary platinum alloys have a miscibility gap at low temperatures, as shown by their phase diagrams (19, 20, 25). Examples of this are given in Figures 26 and 27 for Pt-Ir and Pt-Au, respectively. Similar behaviour is observed for Pt-Co, Pt-Cu and Pt-Rh alloys.

As a consequence, a biphasic structure is expected of each of them. However, this may not occur for various reasons. The phase diagrams refer to equilibrium conditions, which hardly ever correspond to the as-cast conditions. One of the two phases is sometimes present but in low volumetric fraction, due to the chemical composition of the alloy, in which one of the two elements has a low concentration. Furthermore, the thermal treatments may have homogenised the alloy. Finally, the metallographic preparation may not be able to reveal such biphasic structures. Therefore, it is necessary to use other analytical techniques to detect the type and concentration of the alloy phases. Only in specific cases can the biphasic structure be revealed.

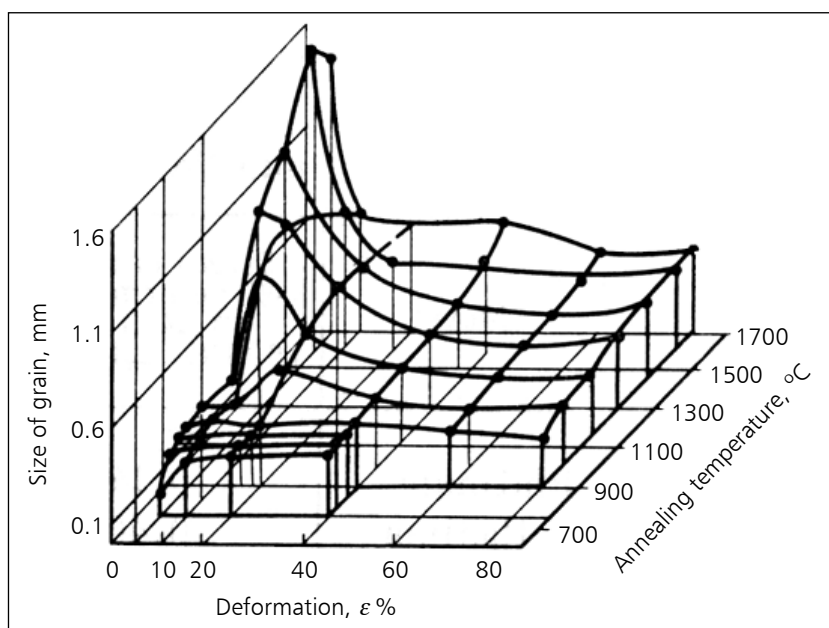


Fig. 18. Recrystallisation diagram of a platinum-rhodium alloy annealed at a set temperature for a given time after a deformation of  $\epsilon$  %. Adapted from (10). By increasing the annealing temperature the grain size increases. During annealing the grain size also increases if the previous deformation is reduced

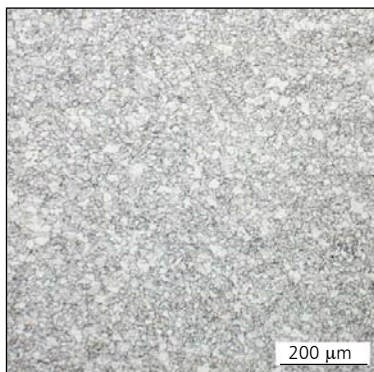


Fig. 19. 60Pt-25Ir-15Rh alloy: from the transverse section of an ingot, after various stages of work hardening and annealing (microhardness  $212 \pm 5 \text{ HV}_{200}$ ). Compare with the as-cast sample shown in Figure 6

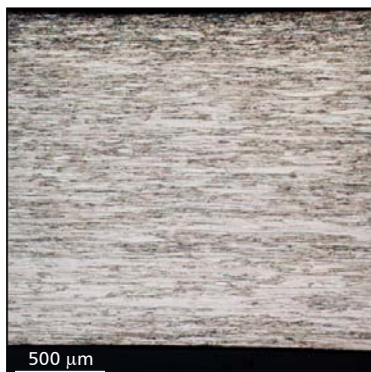


Fig. 20. Pt-5Au alloy: longitudinal section (along the drawing direction) of a drawn cold worked wire (microhardness  $190 \pm 4 \text{ HV}_{200}$ )

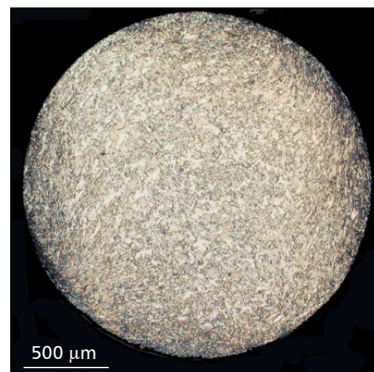


Fig. 21. Pt-5Au alloy: transverse section of the drawn cold worked wire seen in Figure 20 (microhardness  $190 \pm 4 \text{ HV}_{200}$ )

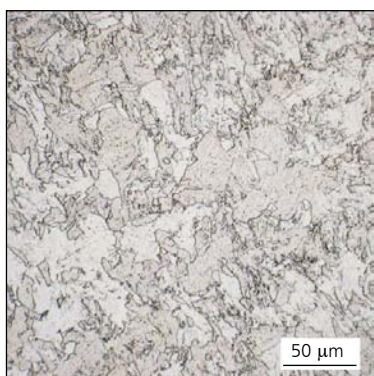


Fig. 22. Pt-5Au alloy: detail of Figure 21 showing the deformation of the grains

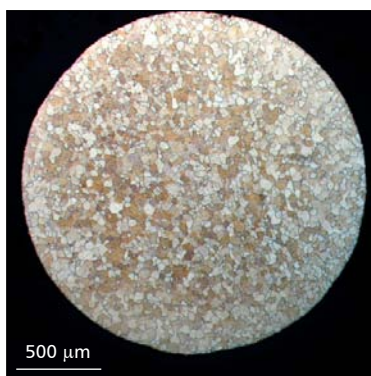


Fig. 23. Pt-5Au alloy: transverse section of the wire seen in Figure 21, after oxygen-propane flame annealing (microhardness  $104 \pm 6 \text{ HV}_{200}$ )

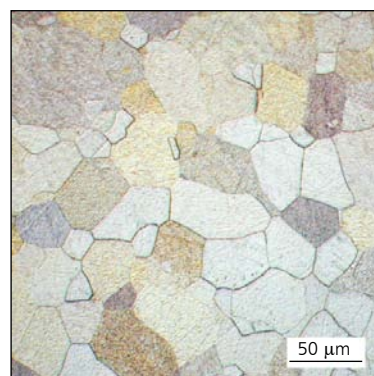


Fig. 24. Pt-5Au alloy: detail of Figure 23, showing the recrystallised grains

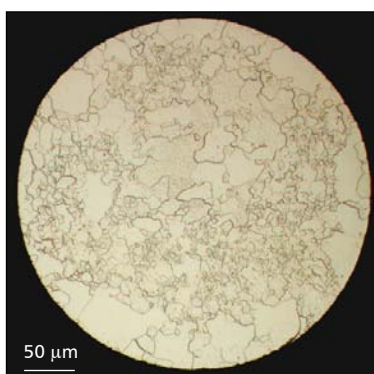


Fig. 25. Pt 99.99% wire: transverse section of the wire after various stages of drawing and annealing (diameter 0.35 mm; microhardness  $65 \pm 3 \text{ HV}_{100}$ )

The best results in working platinum alloys are generally achieved by hot forging the ingot during the first stages of the procedure. Metallography shows the differences between a material that has been cold worked and annealed (Figures 28 and 29 for Pt-5Cu) and a material that has been hot forged (Figures 30 and 31). Hot forging more easily achieves a homogeneous and grain-refined microstructure, free of defects. This is due to the dynamic recrystallisation that occurs during hot forging (26).

#### The Limits of Metallography

Optical metallography is only the first step towards the study of the microstructure of an alloy. A wide variety of analytical techniques can be used alongside

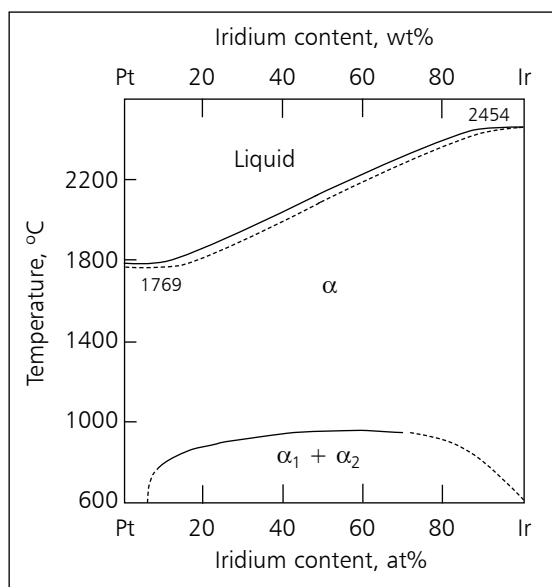


Fig. 26. Pt-Ir phase diagram showing a miscibility gap at low temperatures (20)

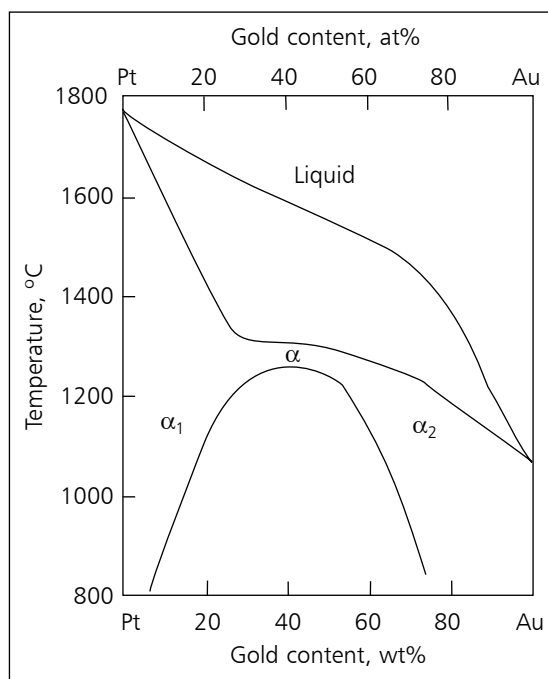


Fig. 27. Pt-Au phase diagram showing a miscibility gap at low temperature (25)

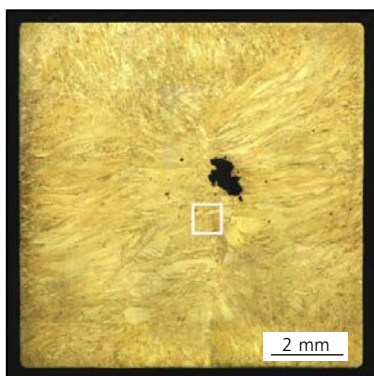


Fig. 28. Pt-5Cu alloy: from a transverse section of a 19 mm × 19 mm ingot, which was rod milled, annealed in a furnace and finished at 10 mm × 10 mm by drawing. The sample shows residual coarse grain microstructure from the as-cast condition and fractures along the bar axis (microhardness  $208 \pm 13$  HV<sub>200</sub>). The small square shows the position of the detail seen in Figure 29

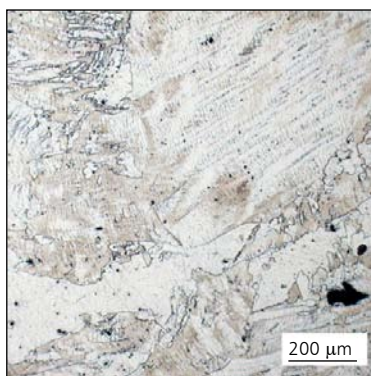


Fig. 29. Pt-5Cu alloy: detail of Figure 28, with coarse grains and small opened cracks evident

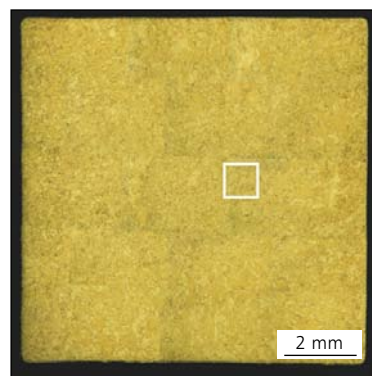
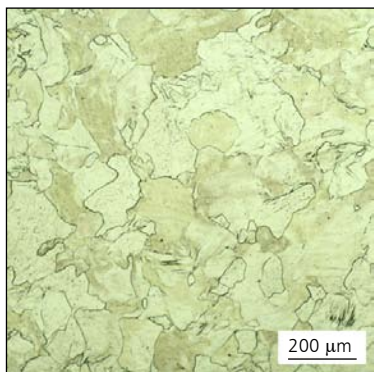


Fig. 30. Pt-5Cu alloy: from a transverse section of a 19 mm × 19 mm bar, which was hot hammered, torch annealed and finished by drawing. The sample has homogeneous microstructure with small grain size (microhardness  $200 \pm 9$  HV<sub>200</sub>). The small square shows the position of the detail seen in Figure 31





*Fig. 31. Pt-5Cu alloy: detail of Figure 30, showing recrystallised grains partially deformed due to the work hardening*

it to provide a far more complete knowledge of the microstructure. One of the most widely used techniques is SEM. In addition to this, EDS allows the relative concentration of the contained chemical elements to be determined, as shown in **Figures 8–10**. Further studies can be performed by X-ray diffraction (XRD), which reveals the different crystal phases present in the alloy.

When working with platinum alloys, often only very small specimens are available, therefore more recent techniques may be required in order to study them. One of these is the focused ion beam (FIB) technique, which can produce microsections of a specimen (27, 28). The microsections are then analysed by other techniques, such as transmission electron microscopy (TEM). In this case the details of microstructure can be detected due to the high spatial resolution of the technique. The crystal structure of the primary and secondary phases can be studied by electron diffraction. Another interesting technique is nano-indentation, performed with micron-sized indenters, which allows hardness measurements to be performed with a spatial resolution far better than that attainable with ordinary micro-indenters. The data obtained from these measurements allows the measurement of fundamental mechanical properties of the alloy, such as the elastic modulus (Young's modulus) (29).

## Conclusions

The metallographic analysis of platinum alloys can be profitably carried out by using a specimen preparation methodology based on the techniques used for gold-based alloys. However, electrochemical etching is required in order to reveal the alloy microstructure and observe it by optical microscopy. A saturated

solution of sodium chloride in concentrated hydrochloric acid can be successfully used for a great many platinum alloys, both in the as-cast condition and after work hardening. Optical metallography provides essential data on the alloy microstructure which can be used in setting up the working procedures. Other techniques can be used alongside it to achieve a more complete knowledge of the material, the effects of the working cycles on it, and to interpret and explain any remaining problems.

## References

- 1 S. Grice, 'Know Your Defects: The Benefits of Understanding Jewelry Manufacturing Problems', in "The Santa Fe Symposium on Jewelry Manufacturing Technology 2007", ed. E. Bell, Proceedings of the 21st Symposium in Albuquerque, New Mexico, USA, 20th–23rd May, 2007, Met-Chem Research Inc, Albuquerque, New Mexico, USA, 2007, pp. 173–211
- 2 P. Battaini, 'Metallography in Jewelry Fabrication: How to Avoid Problems and Improve Quality', in "The Santa Fe Symposium on Jewelry Manufacturing Technology 2007", ed. E. Bell, Proceedings of the 21st Symposium in Albuquerque, New Mexico, USA, 20th–23rd May, 2007, Met-Chem Research Inc, Albuquerque, New Mexico, USA, 2007, pp. 31–65
- 3 "Failure Analysis and Prevention", eds. R. J. Shipley and W. T. Becker, ASM Handbook, Volume 11, ASM International, Ohio, USA, 2002
- 4 G. F. Vander Voort, "Metallography: Principles and Practice", Material Science and Engineering Series, ASM International, Ohio, USA, 1999
- 5 "Metallography and Microstructures", ed. G. F. Vander Voort, ASM Handbook, Volume 9, ASM International, Materials Park, Ohio, USA, 2004
- 6 G. Petzow, "Metallographic Etching", 2nd Edn., ASM International, Ohio, USA, 1999
- 7 T. Piotrowski and D. J. Accinno, *Metallography*, 1977, **10**, (3), 243
- 8 D. Ott and U. Schindler, *Gold Technol.*, 2001, **33**, 6
- 9 "Standard Practice for Microetching Metals and Alloys", ASTM Standard E407, ASTM International, West Conshohocken, Pennsylvania, USA, 2007
- 10 E. M. Savitsky, V. P. Polyakova, N. B. Gorina and N. R. Roshan, "Physical Metallurgy of Platinum Metals", Metallurgiya Publishers, Moscow, Russia, 1975 (in Russian); English translation, Mir Publishers, Moscow, Russia, 1978
- 11 P. Battaini, 'The Metallography of Platinum and Platinum Alloys', in "The Santa Fe Symposium on Jewelry Manufacturing Technology 2010", ed. E. Bell, Proceedings of the 24th Symposium in Albuquerque, New Mexico, USA, 16th–19th May, 2010, Met-Chem Research Inc, Albuquerque, New Mexico, USA, 2010, pp. 27–49

- 12 M. Grimwade, "Introduction to Precious Metals: Metallurgy for Jewelers and Silversmiths", Brynmorgen Press, Brunswick, Maine, USA, 2009
- 13 J. Maerz, 'Platinum Alloy Applications for Jewelry', in "The Santa Fe Symposium on Jewelry Manufacturing Technology 1999", ed. D. Schneller, Proceedings of the 13th Symposium in Albuquerque, New Mexico, USA, 16th–19th May, 1999, Met-Chem Research Inc, Albuquerque, New Mexico, USA, 1999, pp. 55–72
- 14 J. Huckle, 'The Development of Platinum Alloys to Overcome Production Problems', in "The Santa Fe Symposium on Jewelry Manufacturing Technology 1996", ed. D. Schneller, Proceedings of the 10th Symposium in Albuquerque, New Mexico, USA, 19th–22nd May, 1996, Met-Chem Research Inc, Albuquerque, New Mexico, USA, 1996, pp. 301–326
- 15 D. P. Agarwal and G. Raykhtsaum, 'Manufacturing of Lightweight Platinum Jewelry and Findings', in "The Santa Fe Symposium on Jewelry Manufacturing Technology 1996", ed. D. Schneller, Proceedings of the 10th Symposium in Albuquerque, New Mexico, USA, 19th–22nd May, 1996, Met-Chem Research Inc, Albuquerque, New Mexico, USA, 1996, pp. 373–382
- 16 J. Maerz, 'Platinum Alloys: Features and Benefits', in "The Santa Fe Symposium on Jewelry Manufacturing Technology 2005", ed. E. Bell, Proceedings of the 19th Symposium in Albuquerque, New Mexico, USA, 22nd–25th May, 2005, Met-Chem Research Inc, Albuquerque, New Mexico, USA, 2005, pp. 303–312
- 17 R. Lanam, F. Pozarnik and C. Volpe, 'Platinum Alloy Characteristics: A Comparison of Existing Platinum Casting Alloys with Pt-Cu-Co', Technical Articles: Alloys, Platinum Guild International, USA, 1997: <http://www.platinumguild.com/output/page2414.asp> (Accessed on 31 December 2010)
- 18 G. Normandeau and D. Ueno, 'Platinum Alloy Design for the Investment Casting Process', Technical Articles: Alloys, Platinum Guild International, USA, 2002: <http://www.platinumguild.com/output/page2414.asp> (Accessed on 31 December 2010)
- 19 R. F. Vines and E. M. Wise, "The Platinum Metals and Their Alloys", The International Nickel Company, Inc, New York, USA, 1941
- 20 "Handbook of Precious Metals", ed. E. M. Savitsky, Metallurgiya Publishers, Moscow, Russia, 1984 (in Russian); English translation, Hemisphere Publishing Corp, New York, USA, 1989
- 21 K. Vaithinathan and R. Lanam, 'Features and Benefits of Different Platinum Alloys', Technical Articles: Alloys, Platinum Guild International, USA, 2005: <http://www.platinumguild.com/output/page2414.asp> (Accessed on 31 December 2010)
- 22 P. Battaini, *Platinum Metals Rev.*, 2011, **55**, (1), 71
- 23 D. Miller, T. Keraan, P. Park-Ross, V. Husemeyer and C. Lang, *Platinum Metals Rev.*, 2005, **49**, (3), 110
- 24 J. C. McCloskey, 'Microsegregation in Pt-Co and Pt-Ru Jewelry Alloys', in "The Santa Fe Symposium on Jewelry Manufacturing Technology 2006", ed. E. Bell, Proceedings of the 20th Symposium in Nashville, Tennessee, USA, 10th–13th September, 2006, Met-Chem Research Inc, Albuquerque, New Mexico, USA, 2006, pp. 363–376
- 25 "Smithells Metals Reference Book", 7th Edn., eds. E. A. Brandes and G. B. Brook, Butterworth-Heinemann, Ltd, Oxford, UK, 1992
- 26 R. W. Cahn, 'Recovery and Recrystallization', in "Physical Metallurgy", eds. R. W. Cahn and P. Haasen, Elsevier Science BV, Amsterdam, The Netherlands, 1996
- 27 P. R. Munroe, *Mater. Charact.*, 2009, **60**, (1), 2
- 28 E. Bemporad, 'Focused Ion Beam and Nano-Mechanical Tests for High Resolution Surface Characterization: Not So Far Away From Jewelry Manufacturing', in "The Santa Fe Symposium on Jewelry Manufacturing Technology 2010", ed. E. Bell, Proceedings of the 24th Symposium in Albuquerque, New Mexico, USA, 16th–19th May, 2010, Met-Chem Research Inc, Albuquerque, New Mexico, USA, 2010, pp. 50–78
- 29 D. J. Shuman, A. L. M. Costa and M. S. Andrade, *Mater. Charact.*, 2007, **58**, (4), 380

### The Author



Paolo Battaini holds a degree in nuclear engineering and is a consultant in failure analysis for a range of industrial fields. He is responsible for research and development at 8853 SpA in Milan, Italy, a factory producing dental alloys and semi-finished products in gold, platinum and palladium alloys, and is currently a professor of precious metal working technologies at the University of Milano-Bicocca, Italy. Professor Battaini is also a recipient of the Santa Fe Symposium® Ambassador Award and regularly presents at the Santa Fe Symposium® on Jewelry Manufacturing Technology.